



## Using a low-cost drone to assess herbaceous biomass and quality in the Sahelian Rangeland ecosystems

Haftay Hailu Gebremedhin, Paulo Salgado, Cofélas Fassinou & Simon Taugourdeau

**To cite this article:** Haftay Hailu Gebremedhin, Paulo Salgado, Cofélas Fassinou & Simon Taugourdeau (23 Sep 2025): Using a low-cost drone to assess herbaceous biomass and quality in the Sahelian Rangeland ecosystems, African Journal of Range & Forage Science, DOI: [10.2989/10220119.2025.2525418](https://doi.org/10.2989/10220119.2025.2525418)

**To link to this article:** <https://doi.org/10.2989/10220119.2025.2525418>



© 2025 The Author(s). Co-published by NISC Pty (Ltd) and Informa UK Limited, trading as Taylor & Francis Group



Published online: 23 Sep 2025.



[Submit your article to this journal](#)



[View related articles](#)



[View Crossmark data](#)

# Using a low-cost drone to assess herbaceous biomass and quality in the Sahelian Rangeland ecosystems

Haftay Hailu Gebremedhin<sup>1,2\*</sup>, Paulo Salgado<sup>2,3</sup>, Cofélas Fassinou<sup>2</sup> and Simon Taugourdeau<sup>2,3</sup>

<sup>1</sup> College of Agriculture and Environmental Sciences, Haramaya University, Ethiopia

<sup>2</sup> Dispositif partenarial, Pôle Pastoralisme et Zones Sèches, Pôle de recherche de Hann, ISRA, Dakar, Senegal

<sup>3</sup> UMR SELMET, CIRAD, INRAE, Institut Agro University of Montpellier, Montpellier, France

\* Correspondence: [hailuhft418@gmail.com](mailto:hailuhft418@gmail.com)

Existing ways of assessing rangeland plant biomass and nutritional quality mostly rely on field surveys, which are difficult to generalise across plots, along with laboratory-based techniques that entail lengthy pre-processing procedures. As a solution, drones have emerged as a promising tool capable of collecting low-altitude images over expansive areas with minimal effort and cost. Here, we explore the potential of low-cost drone images to estimate the rangeland biomass, and quality of the Sahelian rangeland ecosystem. Model calibration and validation were conducted using a random forest machine learning algorithm, where the response variables were field vegetation samples, and the explanatory variables were derived from drone image outputs. A principal component analysis (PCA) was conducted to explore the multivariate relationships between drone-derived vegetation indices and field-measured biomass and quality attributes. In the validation datasets, the random forest model exhibited relative root mean squared errors (RRMSE) of 31% for fresh mass and 37% for dry mass. The random forest model demonstrated a relatively high prediction accuracy, yielding RRMSE values of 32% for crude protein, 9% for neutral detergent fibre, 8% for acid detergent fibre, and 17% for organic matter digestibility contents. The PCA revealed that the first two components explained 53.3% of the total variance. Overall, these results showed that red, green and blue (RGB) images acquired from low-cost drones can be used to estimate rangeland biomass and quality.

**Keywords:** vegetation quality; rangeland monitoring, photogrammetry, unmanned aerial vehicles

## Introduction

Satellite imaging technologies have become an extremely useful tool for collecting data in various agricultural applications because they allow the acquisition of standardised and repeated information at different spatial and temporal scales (Gillan et al. 2019; Geilpel et al. 2021). However, the major limitations of currently available satellite sensors include high costs, insufficient spatial resolution for identifying the proposed variable, the risk of cloudy scenes, and long revisit periods (Yang et al. 2017).

To address this gap, unmanned aerial vehicles (UAVs), commonly called drones, have become increasingly valuable in various applications, such as vegetation monitoring (Merz and Chapman 2012), agriculture (Marino et al. 2019; Théau et al. 2020), water-quality analyses (Koparan et al. 2019) and soil management (Oliveira et al. 2019). Recent advancements in drone technology and the development of photogrammetric software have led to the production of detailed 3D representations of rangeland vegetation (Barbedo 2019; Barnettson et al. 2020; Lussem et al. 2020; Geilpel et al. 2021). Drones can observe images at centimetre resolution for frequent on-demand deployments yielding imagery on scales sufficiently fine to resolve low-structure rangeland vegetation (Barnetson et al. 2020). When drone images overlap, they can be used to create a 3D model of the observed area (Visockiene et al. 2016). Software is

available that can produce digital surface models (DSM), orthophotos and other related products (Bossoukpe et al. 2021a). Furthermore, vegetation indices offer a quantitative measurement of vegetation features per image pixel (Yeom et al. 2019). Machine learning algorithms, such as Random Forest Regression and Partial Least Squares Regression, have been applied to estimate rangeland plant biomass and quality using highly correlated spectral reflectance data, often outperforming simple linear regression models (Vera-Velez et al. 2023; Zwick et al. 2024). These new tools, along with the imaging products we can create using them, have the potential to address a variety of rangeland management issues (Ogunbuyi et al. 2024).

The Sahel region of Africa forms a transitional zone between the Sahara Desert to the north and more fertile southern regions. Spanning from Senegal in the west to Djibouti in the east (Figure 1), the rangeland is pivotal for pastoralism, contributing significantly to overall food security and the local economy (De Haan et al. 2016). It also provides vital ecological services, including erosion protection, wildlife habitat support and carbon sequestration (Umutoni et al. 2015; Mbow et al. 2020; Gebremedhn et al. 2025).

However, many of these ecosystems are deteriorating due to climate change, drought and desertification (Tagesson et al. 2015; Lo et al. 2022; Wieckowski et al. 2024), as well as

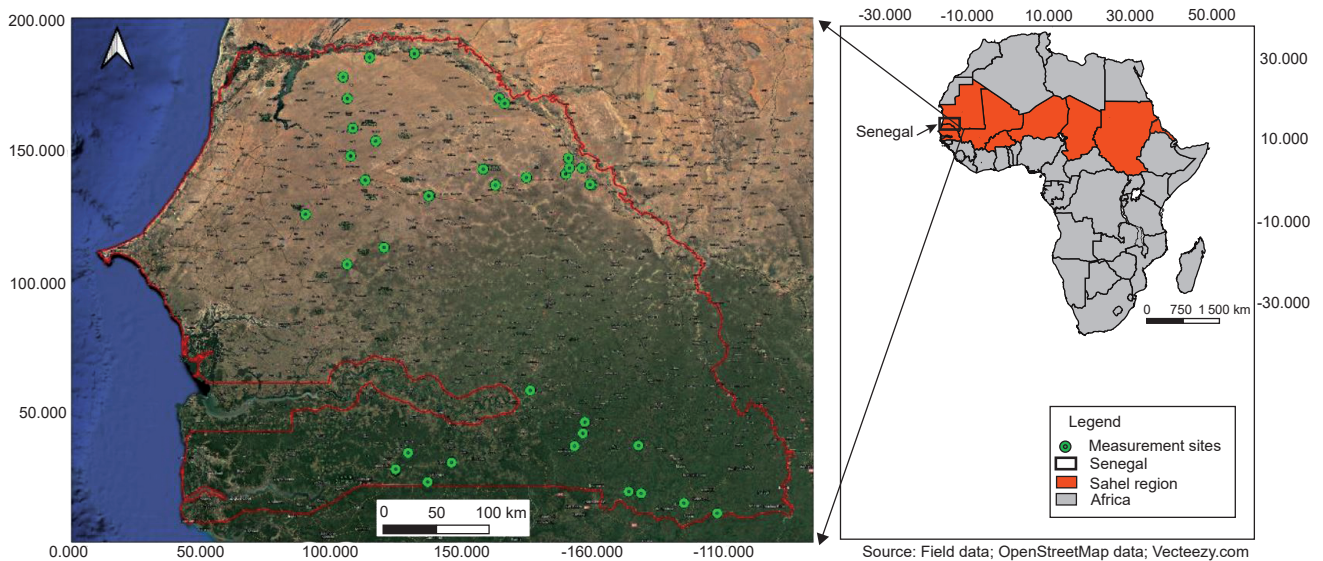


**Figure 1:** Location of study sites

suboptimal grazing management (Gebremedhn et al. 2023). Key parameters for grazing systems in the region are crude protein (CP), neutral detergent fibre (NDF), acid detergent fibre (ADF) and digestible organic matter (DOM) (Barchiesi-Ferrari et al. 2011; Amole et al. 2022). The methods currently used to evaluate plant biomass and quality in these Sahel rangelands involve labour-intensive field surveys, which are often difficult to generalise to larger areas, or laboratory-based techniques that involve time-consuming pre-processing procedures (Escarcha et al. 2018). Sustainable pastoralism also depends on understanding rangeland climate and management practices. However, describing the antecedent conditions of rangeland resources is challenging due to the heterogeneity of grazing landscapes at both micro and macro spatial scales throughout the year. Many pastoralist properties are extensive, making it difficult to detect issues in a timely manner through ground scouting alone (Lo et al. 2022, 2024).

In contrast, high-resolution imagery from drones enables efficient capture of low-altitude images over vast areas (Zhang et al. 2021). This capability has the potential to simplify the estimation of herb biomass and tree community characteristics in the Sahelian rangeland ecosystems (Bossoukpe et al. 2021b; Taugourdeau et al. 2022). However, to the best of the researchers' knowledge, the use of affordable drone technology to assess the quality of rangeland vegetation for livestock feeding in the Sahelian rangelands remains underexplored. Most studies using near-infrared imagery (NIR) have been conducted in temperate rangeland ecosystems, rather than in tropical or arid rangelands (Meng et al. 2022; Wang et al. 2024; Zhu et al. 2024). However, the use of drones equipped with NIR or multispectral cameras remains costly, making them difficult to deploy for many researchers and farmers in low-income settings (Cucho-Padin et al. 2020; Makam et al. 2024). Therefore, this study aimed to assess the feasibility of using a budget-friendly drone equipped with visible red, green and blue (RGB) cameras to estimate herbaceous biomass and

quality in the Senegalese rangeland ecosystem. Specifically, (i) we estimated herbaceous biomass and quality attributes based on RGB imagery outputs using a random forest model; and (ii) we analysed the multivariate relationships between drone-derived indices and vegetation attributes.

## Material and methods

### Description of the study area

The study was carried out in the savanna ecosystem of Senegal located in the Sahel region of West Africa (Figure 1). The region has a unimodal rainfall pattern, with a short rainy season extending from June to October. Annual rainfall ranges from 200 mm in the northern Sahelian zones to 1 200 mm in the southern sub-humid zones, reflecting a clear North–South gradient. Average annual temperatures are 35 °C.

The soil varies across the gradient, with sandy soils dominating the northern sites and ferralitic soils more common in the southern regions (Taugourdeau et al. 2023). Vegetation types represent a diversity of rangeland ecosystems, ranging from open Sahelian steppe with sparse herbaceous cover and almost no trees, to denser wooded savannas with higher vegetation cover. This range of ecological conditions enhances the applicability of the study to broader dryland contexts. The land-use system in the region is mainly pastoral; animal husbandry is completely dependent on natural vegetation. Cattle breeders are nomadic and use most of the land for natural grazing.

### Drone imagery collection

A total of 43 sites were selected along the North–South climatic and ecological gradient. Each site covered 100 m x 100 m (1 ha). Inside each 1 ha site, three wooden triangles, painted in white, were marked out prior to the flight being carried out to delimit the camera images. Flights were conducted using a Parrot ANAFI drone with a PIX4D capture application (<https://www.pix4d.com/product/pix4dcapture>)

using the double grid flight plan. Flight altitude was 80 metres, with 80% front and side overlap at low speed and an 80° camera angle.

The drone surveys were conducted at the end of the growing season, between September and October, coinciding with the flowering stage of most herbaceous species. Flights began in the northern sites (September), where the growing season ends earlier, and progressed southward (late September to October). Flights were performed during daylight hours, with some variability in lighting conditions based on time of day and site accessibility.

### Biomass sampling and collection

Following each drone flight, biomass sampling was conducted within the corresponding 1 ha site. Inside each site one to three 1 m<sup>2</sup> quadrats were distributed randomly to capture intra-site variability. At each site, herbaceous biomass was harvested from the 1 m<sup>2</sup> quadrats, yielding a total of 80 quadrats across all 43 sites.

All herbaceous vegetation within each quadrat was clipped at ground level. Fresh mass (FM) was immediately weighed in the field. Samples were then stored in a plastic bag and later oven-dried at 65 °C to constant weight to obtain dry mass (DM). Data collection was synchronised with the drone flights to ensure that all samples were taken during the peak flowering stage, thereby reducing seasonal error related to differences between flowering and senescence stages.

**Table 1:** Mean and standard deviation (SD) of measured herbaceous biomass, and chemical compositions (quality)

	Vegetation biomass (g/m <sup>2</sup> )		Vegetation chemical composition (%)			
	FM	DM	CP	NDF	ADF	DOM
Mean	506.55	414.25	7.43	69.08	42.58	33.04
SD	211.84	173.41	3.41	9.06	4.94	7.93

ADF = acid detergent fibre  
CP = crude protein  
DM = dry mass  
DOM = digestible organic matter  
FM = fresh mass  
NDF = neutral detergent fibre

**Table 2:** List of vegetation indices used

Acronym	Name	Formula	Source
GR	Normalised difference Green Red index	$(\text{Red} - \text{Green}) / (\text{Red} + \text{Green})$	Bhagat et al. 2020
GB	Normalised difference Blue Green index	$(\text{Green} - \text{Blue}) / (\text{Green} + \text{Blue})$	Bannari et al. 1995
RB	Normalised difference Blue Red index	$(\text{Red} - \text{Blue}) / (\text{Red} + \text{Blue})$	Bossoukpe et al. 2021b
VARI	Visible atmospherically resistant index	$(\text{Green} - \text{Red}) / (\text{Green} + \text{Red} - \text{Blue})$	Gitelson et al. 2002
EXG	Excess of green	$\text{Green} - 0.39 \times \text{Red} - 0.61 \times \text{Blue}$	Barbosa et al. 2019
GLI	Green leaf index	$(2 \times \text{Green} - \text{Red} - \text{Blue}) / (2 \times \text{Green} + \text{Red} + \text{Blue})$	Louhaichi et al. 2001

**Table 3.** Mean and standard deviation (SD) of photogrammetry image processing outputs ( $n = 80$ )

	MH	Hmax	Red	Blue	Green	GR	GB	RB	VARI	EXG	GLI
Mean	0.14	0.42	155.32	65.74	128.52	0.39	0.33	0.40	0.11	27.84	0.07
SD	0.22	1.39	43.78	32.51	32.51	0.18	0.15	0.18	0.10	20.00	0.07

EXG = excess of green  
GB = normalised difference Blue Green Index  
GLI = green leaf index  
GR = normalised difference Green Red Index

Hmax = maximum height  
MH mean height  
RB = normalised difference Blue Red Index  
VARI = visible atmospherically resistant index

### Vegetation quality analysis

To analyse vegetation quality, the DM was ground to 1 mm, then scanned to acquire the spectral signature using a Bruker TANGO OPUS FT-NIR spectrometer. Spectral data were recorded as absorbance (A) using the following equation (Cambou et al. 2016):

$$A = \log 1/R \quad (1)$$

where R is reflectance.

Subsequently, indicators of vegetation quality for livestock feeding including the CP, NDF, ADF, and DOM of the samples were estimated from the samples. These predictions were based on models calibrated by the animal feed laboratory at CIRAD's SELMET Joint Research Unit in Montpellier, France. The models were established with reference to values from vegetation biomass samples collected throughout the savanna ecosystem of Senegal (Table 1).

### Image processing

RGB images were processed with PIX4DMapper (Photogrammetry software <https://www.pix4d.com/>) using Structure from Motion (SfM). SfM is a photogrammetry technique used to obtain reliable data of real-world objects in the environment by creating a variety of 3D spatial models as well as 2D orthomosaics from a set of images. Moreover, six different indices for RGB reflectance use were calculated from the pixel orthophotographs (Table 2).

We used the digital numbers directly when calculating the indices. The mean and standard deviation of the image processing outputs are presented in Table 3.

### Data analysis

Data were analysed using R Statistical Software version 4.2.2 (R Core Team 2022). Model calibration and validation was conducted using a random forest algorithm, with the field samples of vegetation biomass (FM and DM) and quality parameters (CP, NDF, ADF and DOM) as response variables, and drone image output as explanatory variables.

The predictor variables were the heights (average and maximum height), red, green and blue digital numbers, and the six vegetation indices (Table 2).

For each dataset, we randomly split the data into two groups, using two thirds for training (calibration dataset) and one third for validation (validation dataset). To address the unbalanced distribution of FM and DM, we applied a root mean square transformation. For CP, NDF, ADF and DOM, a log transformation was used. We determined the percentage of explained variance to assess how effectively the model fitted on the calibration dataset. In each iteration of the random forest process, 500 regression trees were used. For each tree, six predictor variables were randomly selected from one-third of the calibration dataset. The significance of each predictor variable was evaluated based on mean squared error (MSE) reduction and node purity. Mean reduction in accuracy was calculated by comparing the quality of regression trees with and without the variable. The variable with the highest mean percentage of precision reduction was considered the most important. In regression, node purity refers to the overall reduction of the residual sum of squares when dividing by a single variable, averaged over all trees. This indicates how much the prediction reduces variance.

The calibrated random forest models were used to predict vegetation biomass and chemical compositions for validation sites. These predictions were compared to field measurement values of the validation dataset. Model prediction quality was assessed using root mean squared error (RMSE) and relative RMSE, calculated by dividing RMSE by the mean of measured values (RRMSE). This random validation process

was repeated 100 times, and average values of RMSE and RRMSE were calculated (Figure 2). Additionally, principal component analysis (PCA) was conducted to analyse multivariate relationships between drone-derived indices and vegetation attributes using the *PCA* function from the *FactoMineR* package in R.

## Results

### Vegetation biomass

The average FM was 506.55 g m<sup>-2</sup>, and the average DM was 211.84 g m<sup>-2</sup> (Table 1). The random forest model exhibited a percentage of explained variance of 67.09% for FM and 58.78% for DM. Notably, the GLI region's wavebands and the height (both mean and maximum) emerged as the most important variables in estimating both FM and DM (Figure 3). On the validation dataset, the root mean square error (RMSE) was 117.36 g m<sup>-2</sup> (RRMSE = 0.31) for FM and 58.88 g m<sup>-2</sup> (RRMSE = 0.37) for DM (Table 4).

### Vegetation quality

The average vegetation chemical compositions are presented in Table 1. The random forest model explained 32.21%, 27.09%, 15.26% and 23.18% of the variance for CP, NDF, ADF and DOM, respectively (Table 4). Wavebands in the blue, green and red regions contributed mainly to the estimation of CP content, wavebands in the blue, green regions and Hmax to the estimation of NDF, wavebands in the blue GB and GR regions to the estimation of ADF, and wavebands in the blue, green and red regions to the

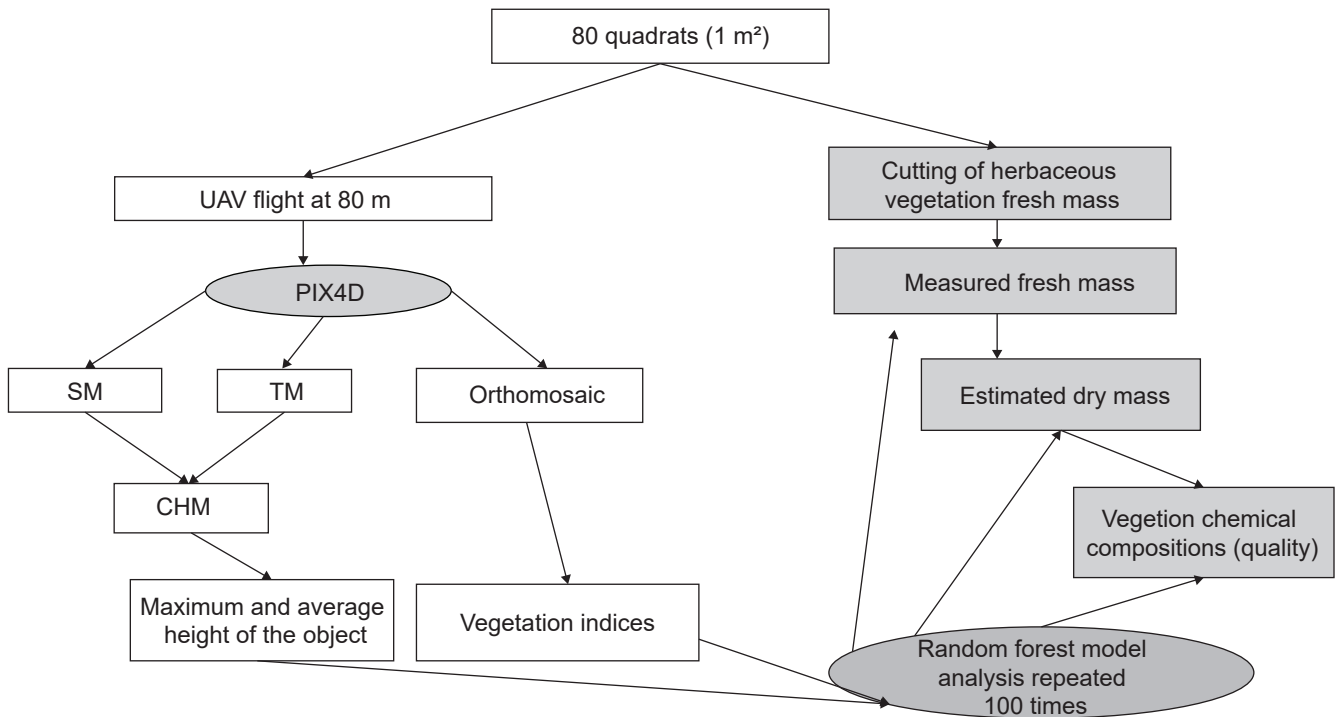


**Figure 2:** Data processing and analysis approach used in this work. The study was conducted on 80 quadrates. The white boxes show the data processing of the drone images. The grey boxes depict the sampling and analysis of vegetation biomass, and chemical composition, from the field sites. The green box represents the machine learning algorithm used for model calibration and validation

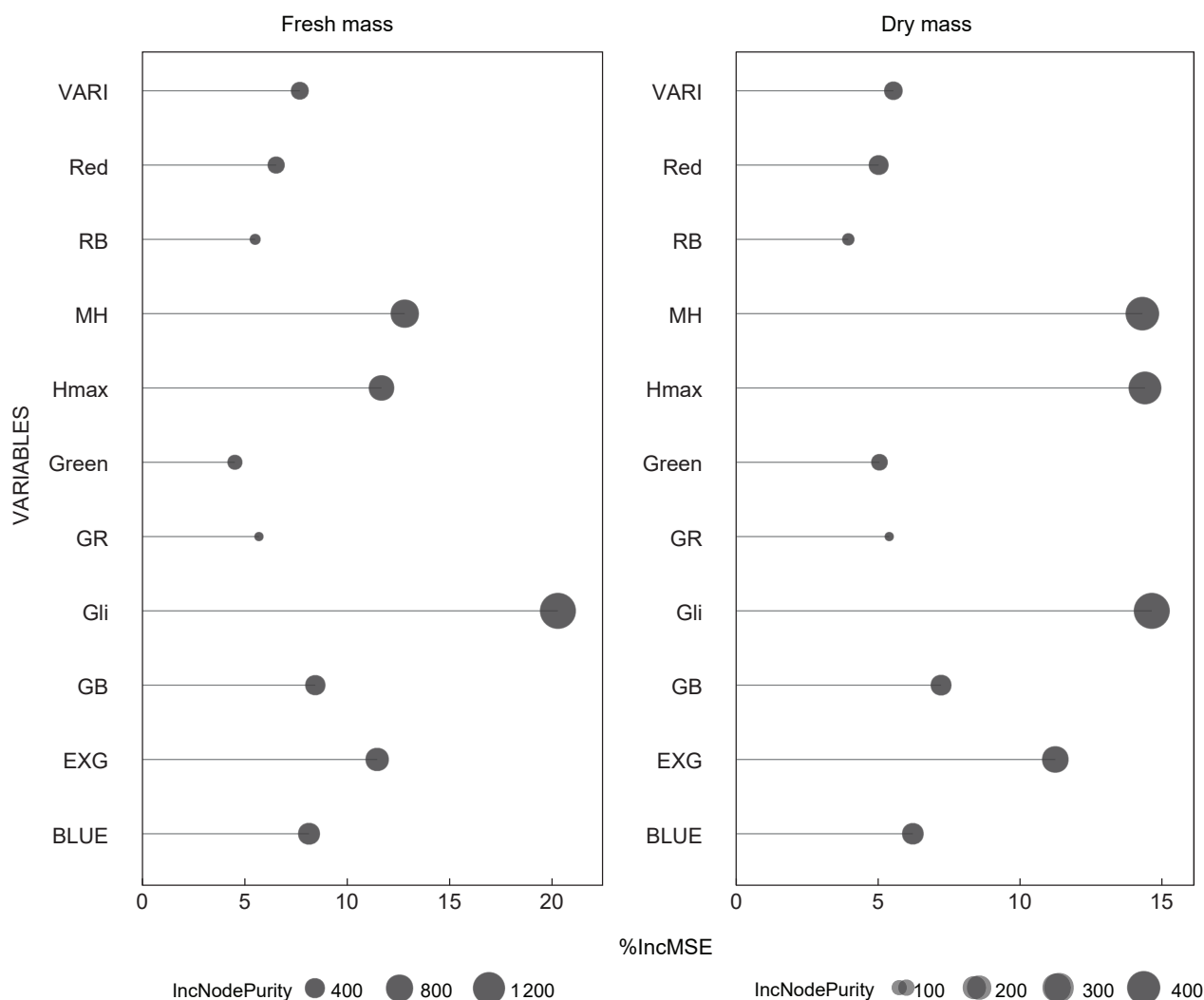


**Figure 3:** Important variables for the prediction of fresh and dry mass

EXG = excess of green

GB = normalised difference Blue Green Index

GLI = green leaf index

GR = normalised difference Green Red Index

%IncMSE = percent increase in Mean Squared Error

IncNodePurity = total decrease in node impurity refers to the reduction in residual sum of squares. The variable with the largest total decrease in %IncMSE and the highest IncNodePurity (represented by lime green dots on the map, Figure 1) is considered the most important

Hmax = maximum height

MH = mean height

RB = normalised difference Blue Red Index

VARI = visible atmospherically resistant index

**Table 4:** Result of random forest model calibration and validation quality indicators

	Forage biomass		Forage chemical composition (quality)				
	FM	DM	DM	CP	NDF	ADF	DOM
RF	67.09	0.5878	0.5878	32.21	27.09	15.26	23.18
$R^2$ test	0.58	0.48	0.48	0.27	0.24	0.21	0.19
RMSE	117.36	58.88	58.88	2.35	6.27	3.39	5.52
RRMSE	0.31	0.37	0.37	0.32	0.09	0.08	0.17

ADF = acid detergent fibre (%)

CP = crude protein (%)

DM = dry mass ( $\text{g m}^{-2}$ )

DOM = digestible organic matter (%)

$R^2$  test =  $R^2$  of the model between predicted and measured values based on the validation dataset

RF = percentage of variation explained by the random forest model on the calibration dataset

RRMSE = relative root-mean-square error

FM = fresh mass ( $\text{g m}^{-2}$ )

NDF = neutral detergent fibre (%)

RMSE = root-mean-square error

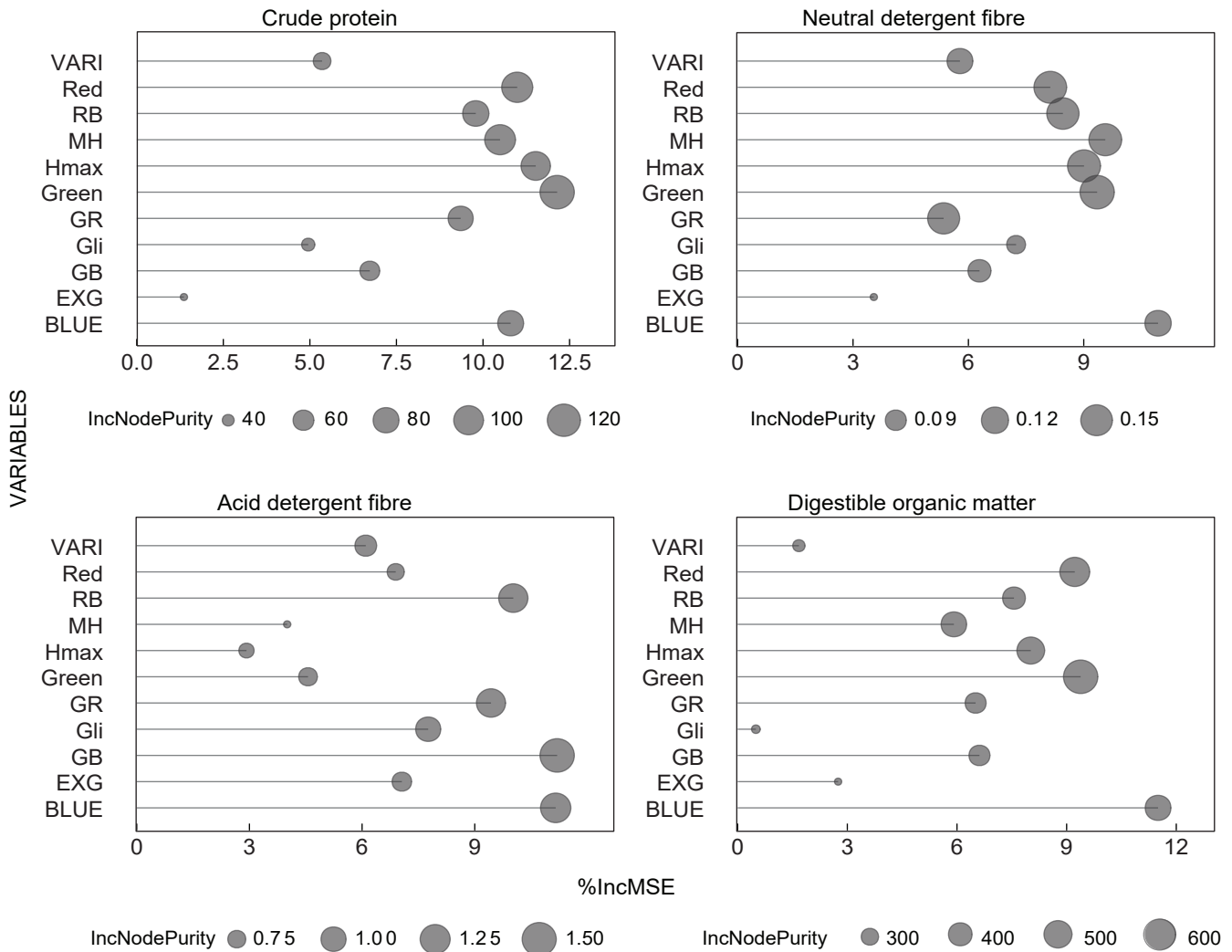


**Figure 4:** Important variables for the prediction of vegetation quality

EXG = excess of green

GB = normalised difference Blue Green Index

GLI = green leaf index

GR = normalised difference Green Red Index

%IncMSE = percent increase in Mean Squared Error

IncNodePurity = total decrease in node impurity refers to the reduction in residual sum of squares. The variable with the largest total decrease in %IncMSE and the highest IncNodePurity (represented by lime green dots on the map figure) is considered the most important

Hmax = maximum height

MH = mean height

RB = normalised difference Blue Red Index

VARI = visible atmospherically resistant index

estimation of DOM (Figure 4). On the validation dataset, the RMSE for CP was 2.35% (RRMSER = 0.32), for NDF it was 6.27% (RRMSER = 0.09), for ADF it was 3.39% (RRMSER = 0.08) and for DOM it was 5.52% (RMSE = 0.17) (Table 4).

Multivariate relationships between drone indices and vegetation attributes

The PCA revealed that the first two principal components accounted for 53.3% of the total variance, with Dimension 1 (32.2%) primarily capturing variation in drone-derived indices and Dimension 2 (21.1%) representing variability in vegetation attributes (Table 5).

Additionally, the PCA biplot (Figure 5) revealed two distinct variable groups, highlighting the potential of low-cost drone imagery to estimate vegetation biomass and quality. The red

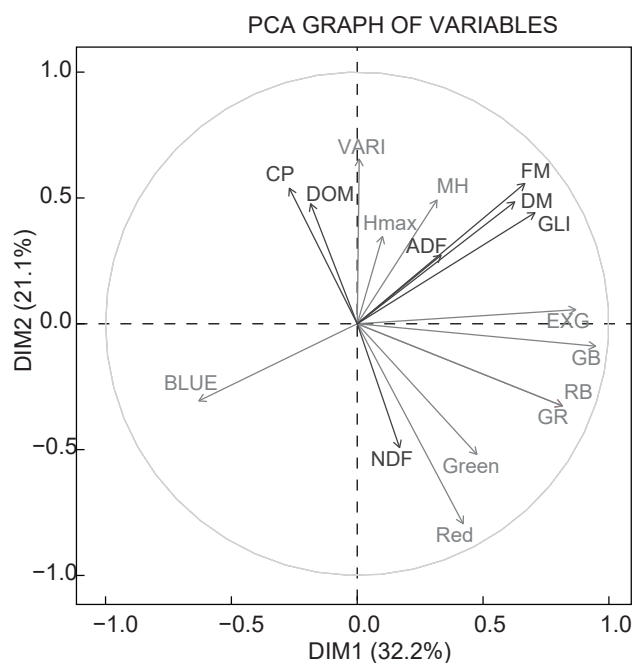
cluster includes drone-derived indices, primarily aligned with Dimension 1, indicating this component captures variation from image-based metrics. The green cluster represents vegetation biomass and quality attributes, more aligned along Dimension 2.

## Discussion

FM predictions showed more accurate predictions compared to DM, as the spectral signals observed from the sensor may have been a more direct measurement of plant FM than DM (Figure 6). The prediction error values for FM and DM were 31% and 37%, respectively. In the same study area, Taugourdeau et al. (2022) reported better prediction accuracy

**Table 5:** Eigenvalues, variance explained, and cumulative variance for principal components between drone-indices and vegetation attributes

Component	Eigenvalue	%Variance explained	Cumulative %
1	5.47	32.19	32.19
2	3.58	21.08	53.26
3	2.91	17.09	70.35
4	2.09	12.28	82.63
5	1.19	7.01	89.65
6	0.81	4.79	94.43
7	0.44	2.62	97.05
8	0.18	1.08	98.13
9	0.15	0.88	99.01
10	0.08	0.44	99.45
11	0.04	0.22	99.67
12	0.03	0.15	99.83
13	0.02	0.11	99.94
14	0.01	0.06	99.99
15–17	< 0.01	~0.00	100.00

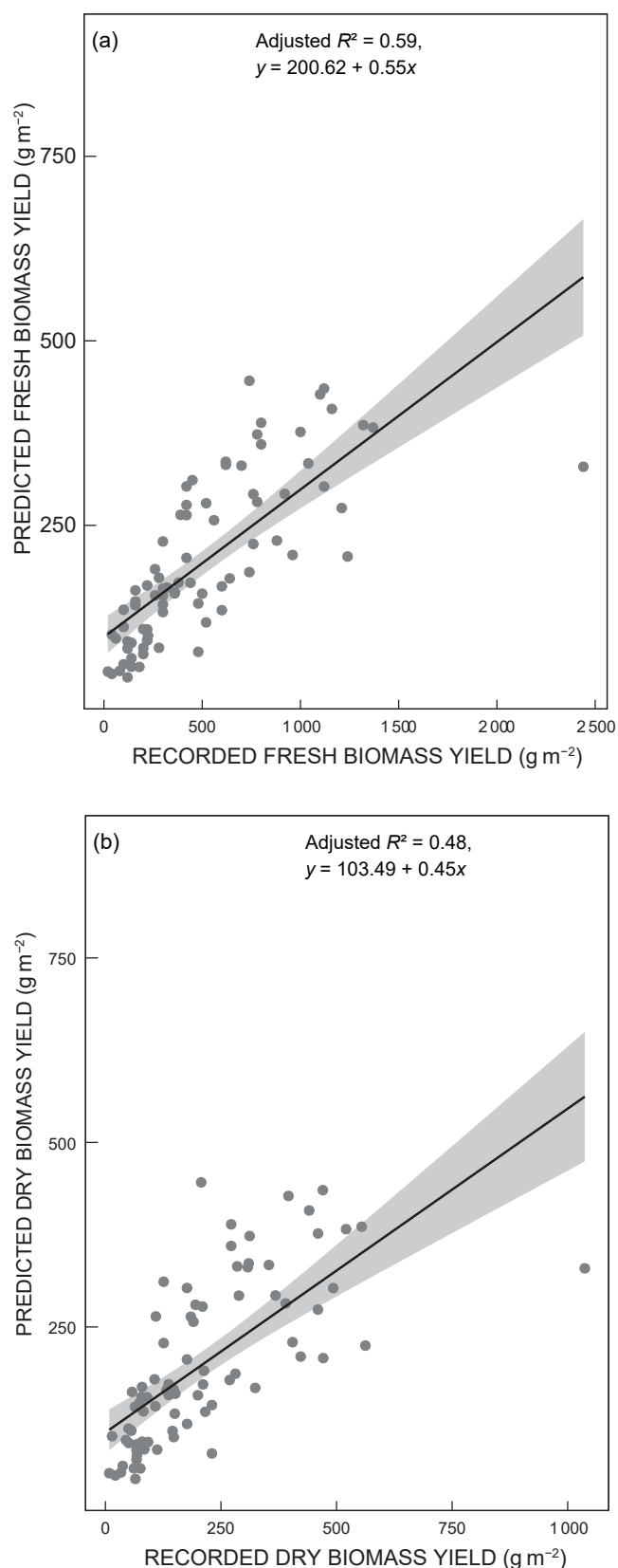
**Figure 5:** PCA biplot of drone-derived indices and vegetation attributes

Grey vectors indicate variables derived from drone imagery:

EXG = excess of green  
 GB = normalised difference Blue Green Index  
 GLI = green leaf index  
 GR = normalised difference Green Red Index  
 Hmax = maximum height  
 MH = mean height  
 RB = normalised difference Blue Red Index  
 VARI = visible atmospherically resistant index

Black vectors represent vegetation biomass and quality variables:

ADF = acid detergent fibre (%)  
 CP = crude protein (%)  
 DM = dry mass (g m<sup>-2</sup>)  
 DOM = digestible organic matter (%)  
 FM = fresh mass (g m<sup>-2</sup>)  
 NDF = neutral detergent fibre (%)

**Figure 6:** Scatterplots showing (a) the measured and (b) predicted plots for fresh mass and dry mass, respectively

for DM, at around 25% error. The distribution of biomass yield estimates showed a higher tendency towards overestimation and underestimation for both the FM and DM parameters.

The height variables (average and maximum height) derived from the DSM showed persistently important for estimating both FM and DM. This finding was in line with the study by Taugourdeau et al. (2022), which reported that the height variables obtained from a 3D model were among the top variables for estimating vegetation FM and DM. In addition, the GLI and EXG vegetation indices were the most important variables for estimating FM and DM. Similarly (Bendig et al. 2014) reported that GLI and EXG were two of the most important variables for estimating vegetation FM and DM. This indicates that the height variables (average and maximum height) obtained from DSM and the vegetation indices obtained from RGB images should be considered when predicting FM and DM using a low-cost drone camera.

The random forest model estimated CP content with an error of 32%. This result was relatively low compared with the result obtained by Năsi et al. (2018), who reported an error of 12%. Durante et al. (2014) reported an even smaller prediction error when estimating CP (10%). However, the random forest model achieved relatively high prediction accuracy, at 9% and 8% error, for NDF and ADF contents, respectively. These results were comparable to those reported by Starks et al. (2004), who found an accuracy of 10% for NDF and Pullanagari et al. (2012), who reported an accuracy of 7% for ADF, which assisted in data collection with a drone-borne hyperspectral camera. Additionally, the prediction error for DOM content was 17%. In contrast, Pullanagari et al. (2012) achieved high prediction accuracy (5% error) for DOM content in mixed pastures (i.e. commercial New Zealand pastures), using a portable spectrometer.

The green, red and blue bands mainly contributed to estimating CP content. In line with this finding, Fava et al. (2009) reported that the red band was known to be strongly correlated with leaf chlorophyll and CP content. Wavebands in the blue and green regions and Hmax were the most important variables to NDF content. Moreover, the blue, GR and GB bands were the most important variables for estimating ADF, while the blue, green and red bands were important for estimating DOM content. To the authors' knowledge, no reference studies have been conducted using low-cost drone cameras to compare vegetation quality. Our work was based solely on the RGB bands and the extracted vegetation indices, but infrared indices are known for vegetation nutritional quality analysis (Bhagat et al. 2020), as these characteristics indicate the absorption of radiation at short wavelengths (Curran 1989).

Furthermore, the random forest model precession (adjusted  $R^2$ ) for FM ( $R^2 = 59$ ) and DM ( $R^2 = 48$ ) biomass was relatively good in the validation datasets, with higher variance of 67.09% for FM and 58.78% for DM in the calibration datasets. In contrast, the random forest model did not achieve satisfactory adjusted  $R^2$  (all under 0.27) in the validation dataset (Table 4) and low variance (all under 32%) in the calibration datasets for the vegetation quality parameters (Table 4). Many examples in the literature (Pullanagari et al. 2018; Bhagat et al. 2020; Geipel 2021) support that the generalisability of a model depends on many factors, such as

the nature of the data, the degree of variation between the environments in which the calibrations are performed, and the size and quality of the calibration data. The low  $R^2$  results in our study might therefore have been due to the small sample size ( $N = 80$ ) in the calibration dataset, one third of which was used for the validation dataset. In support of this, Năsi et al. (2018) found that large datasets were more favourable than models calibrated on smaller datasets. Furthermore, increasing the spectral resolution of drone captors could also be a solution to increase precision. However, the price of high-resolution drones is quite expensive and unaffordable for use in developing countries such as those in the Sahel region.

Furthermore, the PCA demonstrated clear multivariate relationship between drone-derived vegetation indices and field measured biomass and quality attributes. The PCA revealed that the first two components explained 53.3% of the total variance in drone-derived indices and vegetation attributes. Specifically, Component 1 (Dimension 1) explained 32.2% of the variance (eigenvalue = 5.47), while Component 2 (Dimension 2) accounted for 21.1% (eigenvalue = 3.58). The remaining components explained increasingly smaller portions of variance, with Component 3 contributing 17.1%, and Components 4 and beyond each contributing less than 13% (see Table 5). Additionally, the PCA biplot (Figure 5) revealed two distinct clusters of variables. The first cluster, represented in red, includes variables derived from low-cost drone imagery: MH, Hmax, and spectral indices such as GR, GB, RB, VARI, EXG and GLI. These variables predominantly align with the positive axis of Dimension 1, indicating that this component is largely influenced by drone-based vegetation structure and indices indicators. In contrast, the second cluster, shown in green, includes vegetation biomass and quality attributes: FM, DM, CP, NDF, ADF and DOM. These variables are more dispersed along Dimension 2, suggesting this component captures a distinct gradient in vegetation biomass and quality indicators. The clustering patterns support the potential utility of low-cost drone imagery for estimating key indicators of vegetation productivity and forage quality, offering a scalable approach for rangeland monitoring and management.

## Conclusion

Our results showed that herbaceous biomass (FM and DM), and forage qualities (CP, NDF, ADF and DOM) can be estimated using drone-derived red, green and blue (RGB) imagery combined with a random forest model. The model achieved relative root mean squared errors of 31% FM and 37% for DM, 32% for CP, 9% for NDF, 8% for ADF and 17% for DOM, respectively. Additionally, PCA revealed that the first two dimensions explained 53.3% of the total variance in the drone-derived indices, biomass and quality parameters. This suggests low-cost drone systems offer promising potential for supporting rangeland monitoring and management with less effort. However, certain limitations must be acknowledged. Drone-based estimation can be affected by vegetation density, where overlapping canopies may obscure ground cover, reducing prediction accuracy. Additionally, variable lighting conditions, flight angle and camera resolution can introduce noise into the data. These factors highlight the importance of standardised flight

protocols and post-processing techniques to minimise error. Moreover, plant structural diversity and species composition can influence reflectance patterns, which may affect model performance across different rangeland types. Future studies should explore how this approach performs in ecosystems with denser or more heterogeneous vegetation structures. Finally, while our results are promising, they are based on a limited sample size, and further studies with broader spatial and temporal coverage are needed. Expanding this approach to other dryland regions could enhance biomass and quality estimation accuracy and broaden its applicability across diverse rangeland systems.

**Author contributions** — HHG: conceptualisation; data curation; formal analysis; investigation; methodology; software; validation; visualisation; writing (original draft); writing (review and editing). ST and PS: Conceptualisation; data curation; funding acquisition; investigation; methodology; project administration; resources; supervision; writing – review and editing. CF: Formal analysis; editing.

**Conflict of interest statement** — The authors declare no conflict of interest.

**Availability of data and material** — Data are available upon request from the authors.

**Acknowledgements** — This research was supported by the New Zealand Government as part of the Global Research Alliance on Agricultural Greenhouse Gases initiative, as well by the Carbon Sequestration and Greenhouse Gas Emissions in (Agro) Sylvopastoral Ecosystems in the Sahelian CILSS States (CaSSECS) project [FOOD/2019/410-169], supported by the European Union under the Development Smart Innovation through Research in Agriculture (DeSIRA) Initiative. The opinions expressed in this article are not necessarily those of the New Zealand Government and European Union. We thank all the staff of CRZ (Centre de Recherche Zootechnique) in Senegal and the community for their assistance during field data collection. The authors would also like to acknowledge the reviewers and editor for their comments, which helped improve the manuscript greatly.

## ORCID IDS

Hafay Hailu Gebremedhin — <https://orcid.org/0000-0002-9615-114X>

Paulo Salgado — <https://orcid.org/0000-0003-1815-6604>

Cofélas Fassinou — <https://orcid.org/0000-0002-9509-1317>

Simon Taugourdeau — <https://orcid.org/0000-0001-6561-3228>

## References

Amole T, Augustine A, Balehegn M, Adesogoan A. 2022. Livestock feed resources in the West African Sahel. *Agronomy Journal* 114: 26–45. <https://doi.org/10.1002/agj2.20955>

Bannari A, Morin D, Bonn F, Huete AR. 1995. A review of vegetation indices. *Remote Sensing Reviews* 13: 95–120. <https://doi.org/10.1080/02757259509532298>

Barbosa BDS, Ferraz GAS, Gonçalves LM, Marin DB, Maciel DT, Ferraz PFP, Rossi G. 2019. RGB Vegetation indices applied to grass monitoring: a qualitative analysis. *Agronomy Research* 17: 349–357. <https://doi.org/10.1515/AR.19.119>

Barbedo JGA. 2019. A review on the use of unmanned aerial vehicles and imaging sensors for monitoring and assessing plant stresses. *Drones* 3: 40. <https://doi.org/10.3390/drones3020040>

Barchiesi-Ferrari C, Alomar D, Miranda H. 2011. Pepsin-cellulase

digestibility of pasture silages: effects of pasture type, maturity stage, and variations in the enzymatic method. *Chilean Journal of Agricultural Research* 71: 249–257. <https://doi.org/10.4067/s0718-58392011000200010>

Barnetson J, Phinn S, Scarth P. 2020. Estimating plant pasture biomass and quality from UAV imaging across Queensland's rangelands. *AgriEngineering* 2: 523–543. <https://doi.org/10.3390/agriengineering2040035>

Bendig J, Bolten A, Bennertz S, Broscheit J, Eichfuss S, Bareth G. 2014. Estimating biomass of barley using crop surface models (CSMs) derived from UAV-based RGB imaging. *Remote Sensing* 6: 10395–10412. <https://doi.org/10.3390/rs61110395>

Bhagat V, Kada A, Kumar S. 2020. Analysis of remote sensing based vegetation indices (VIs) for unmanned aerial system (UAS): A Review. *Remote Sensing of Land* 3: 58–73. <https://doi.org/10.21523/gcjl.19030202>

Bossoukpe M, Faye E, Ndiaye O, Diatta S, Diatta O, et al. 2021a. Low-cost drones help measure tree characteristics in the Sahelian Savanna. *Journal of Arid Environments* 187: 104449. <https://doi.org/10.1016/j.jaridenv.2021.104449>

Bossoukpe M, Ndiaye O, Diatta O, Diatta S, Audebert A, et al. 2021b. Unmanned aerial vehicle for the assessment of woody and herbaceous phytomass in Sahelian savanna. *Revue d'Élevage et de Médecine Vétérinaire des Pays Tropicaux* 74: 199–205 <https://doi.org/10.19182/remvt.36802>

Cambou A, Cardinael R, Kouakoua E, Villeneuve M, Durand C, Barthès BG. 2016. Prediction of soil organic carbon stock using visible and near infrared reflectance spectroscopy (VNIRS) in the Field. *Geoderma* 261: 151–159. <https://doi.org/10.1016/j.geoderma.2015.07.007>

Cucho-Padin G, Loayza H, Palacios S, Balcazar M, Carbajal M, Quiroz R. 2020. Development of low-cost remote sensing tools and methods for supporting smallholder agriculture. *Applied Geomatics* 12: 247–263. <https://doi.org/10.1007/s12518-019-00292-5>

Curran PJ. 1989. Remote sensing of foliar chemistry. *Remote Sensing of Environment* 30: 271–278. [https://doi.org/10.1016/0034-4257\(89\)90069-2](https://doi.org/10.1016/0034-4257(89)90069-2)

De Haan C, Dubern E, Garancher B, Quintero C. 2016. *Pastoralism Development in the Sahel: A Road to Stability?* World Bank. <http://hdl.handle.net/10986/24228>

Durante M, Oesterheld M, Piñeiro G, Vassallo MM. 2014. Estimating forage quantity and quality under different stress and senescent biomass conditions via spectral reflectance. *International Journal of Remote Sensing* 35: 2963–2981. <https://doi.org/10.1080/01431161.2014.894658>

Escarcha J, Lassa J, Zander K. 2018. Livestock under climate change: a systematic review of impacts and adaptation. *Climate* 6: 54. <https://doi.org/10.3390/cli6030054>

Fava F, Colombo R, Bocchi S, Meroni M, Sitzia M, Fois N, Zucca C. 2009. Identification of hyperspectral vegetation indices for Mediterranean pasture characterization. *International Journal of Applied Earth Observation and Geoinformation* 11: 233–243. <https://doi.org/10.1016/j.jag.2009.02.003>

Gebremedhn HH, Ndiaye O, Mensah S, Fassinou C, Taugourdeau S, Tagesson T, Salgado P. 2023. Grazing effects on vegetation dynamics in the savannah ecosystems of the Sahel. *Ecological Processes* 12: 54. <https://doi.org/10.1186/s13717-023-00468-3>

Gebremedhn HH, Taugourdeau S, Mensah S, Lydie C-L, Tagesson T, Moulin P, Ndiaye O, Wieckowski A, Salgado P. 2025. Grazing affects soil organic carbon stocks directly and indirectly through herbaceous species diversity in Sahelian savanna ecosystems. *Land Degradation and Development* 34: 2636–2651. <https://doi.org/10.1002/ldr.5580>

Geipel J, Bakken AK, Jørgensen M, Korsæth A. 2021. Forage yield and quality estimation by means of UAV and hyperspectral imaging. *Precision Agriculture* 22: 1437–1463. <https://doi.org/10.1007/s11119-021-09790-2>

- Gillan, JK, McClaran MP, Swetnam TL, Heilman P. 2019. Estimating forage utilization with drone-based photogrammetric point clouds rangeland ecology & management estimating forage utilization with drone-based photogrammetric point clouds. *Rangeland Ecology & Management* 72: 575–585. <https://doi.org/10.1016/j.rama.2019.02.009>
- Gitelson A, Kaufman YJ, Stark R, Rundquist D. 2002. Novel Algorithms for Remote Estimation of Vegetation Fraction. *Remote Sensing of Environment* 80: 76–87. [https://doi.org/10.1016/S0034-4257\(01\)00289-9](https://doi.org/10.1016/S0034-4257(01)00289-9)
- Koparan C, Koc AB, Privette CV, Sawyer CB. 2019. Autonomous in situ measurements of noncontaminant water quality indicators and sample collection with a UAV. *Water* 11: 604. <https://doi.org/10.3390/w11030604>
- Lo A, Diouf AA, Diedhiou I, Bassène CDE, Leroux L, Tagesson T, Fensholt R, Hiernaux P, Mottet A, Taugourdeau S, Ngom D, Touré I, Ndao B, Sarr MA. 2022. Dry season forage assessment across senegalese rangelands using earth observation data. *Frontiers in Environmental Science* 10: 1–15. <https://doi.org/10.3389/fenvs.2022.931299>
- Lo A, Diouf AA, Leroux L, Tagesson T, Fensholt R, Mottet A, Bonnal L, Diedhiou I. 2024. Remote sensing-based assessment of dry-season forage quality for improved rangeland management in Sahelian ecosystems. *Rangeland Ecology and Management* 96: 94–104. <https://doi.org/10.1016/j.rama.2024.05.009>
- Louhaichi M, Borman MM, Johnson DE. 2001. Spatially located platform and aerial photography for documentation of grazing impacts on wheat. *Geocarto International* 16: 65–70. <https://doi.org/10.1080/10106040108542184>
- Lussem U, Schellberg J, Bareth G. 2020. Monitoring forage mass with low-cost UAV data : case study at the Rengen Grassland Experiment. *PFG – Journal of Photogrammetry, Remote Sensing and Geoinformation Science* 88: 407–422. <https://doi.org/10.1007/s41064-020-00117-w>
- Makam S, Komatineni BK, Meena SS, Meena U. 2024. Unmanned aerial vehicles (UAVs): an adoptable technology for precise and smart farming. *Discover Internet of Things* 4: 12. <https://doi.org/10.1007/s43926-024-00066-5>
- Marino S, Ahmad U, Ferreira MI, Alvino A. 2019. Evaluation of the effect of irrigation on biometric growth, physiological response, and essential oil of *Mentha spicata* (L.). *Water* 11: 2264. <https://doi.org/10.3390/w11112264>
- Mbow C, Halle M, El Fadel R, Thiaw I. 2020. Land resources opportunities for a growing prosperity in the Sahel. *Current Opinion in Environmental Sustainability* 48: 85–92. <https://doi.org/10.1016/j.cosust.2020.11.005>
- Meng B, Zhang Y, Yang Z, Lv Y, Chen J, Li M, Sun Y, Zhang H, Yu H, Zhang J, Lian J, He M, Li J, Yu H, Chang L, Yi S. 2022. Mapping grassland classes using unmanned aerial vehicle and MODIS NDVI data for temperate grassland in Inner Mongolia, China. *Remote Sensing* 14: 2094. <https://doi.org/10.3390/rs14092094>
- Merz T, Chapman, S. 2012. Autonomous unmanned helicopter system for remote sensing missions in unknown environments. *The International Archives of the Photogrammetry, Remote Sensing and Spatial Information Sciences* 38: 143–148. <https://doi.org/10.5194/isprsarchives-xxxviii-1-c22-143-2011>
- Näsi R, Viljanen N, Kaivosoja J, Alhonoja K, Hakala T, Markelin L, Honkavaara E. 2018. Estimating biomass and nitrogen amount of barley and grass using UAV and aircraft based spectral and photogrammetric 3D features. *Remote Sensing* 10: 1–32. <https://doi.org/10.3390/rs10071082>
- Ogungbuyi MG, Mohammed C, Fischer AM, Turner D, Whitehead J, Harrison MT. 2024. Integration of drone and satellite imagery improves agricultural management agility. *Remote Sensing* 16: 4688. <https://doi.org/10.3390/rs16244688>
- Oliveira RA, Näsi R, Niemeläinen O, Nyholm L, Alhonoja K, Kaivosoja J, Viljanen N, Hakala T, Nezami S, Markelin L, Jauhainen L, Honkavaara E. 2019. Assessment of RGB and hyperspectral UAV remote sensing for grass quantity and quality estimation. *International Archives of the Photogrammetry, Remote Sensing and Spatial Information Sciences* 42: 489–494. <https://doi.org/10.5194/isprs-archives-XLII-2-W13-489-2019>
- Pullanagari RR, Yule IJ, Tuohy MP, Hedley MJ, Dynes RA, King WM. 2012. In-field hyperspectral proximal sensing for estimating quality parameters of mixed pasture. *Precision Agriculture* 13: 351–369. <https://doi.org/10.1007/s11119-011-9251-4>
- Pullanagari RR, Kereszturi G, Yule I. 2018. Integrating airborne hyperspectral, topographic, and soil data for estimating pasture quality using recursive feature elimination with random forest regression. *Remote Sensing* 10: 1117. <https://doi.org/10.3390/rs10071117>
- R Core Team. 2022. *R: a language and environment for statistical computing* (4.2.2). Vienna: R Foundation for Statistical Computing. <https://www.R-project.org/>
- Starks PJ, Coleman SW, Phillips WA. 2004. Determination of forage chemical composition using remote sensing. *Journal of Range Management* 57: 635–640. [https://doi.org/10.2111/1551-5028\(2004\)057\[0635:dofccu\]2.0.co;2](https://doi.org/10.2111/1551-5028(2004)057[0635:dofccu]2.0.co;2)
- Tagesson T, Fensholt R, Guio I, Rasmussen MO, Huber S, Mbow C, Garcia M, Horion S, Sandholt, Holm-Rasmussen B, Götsche FM, Ridler ME, Olén N, Olsen JL, Ehammer A, Madsen M, Olesen FS, Ardö J. 2015. Ecosystem properties of semiarid savanna grassland in West Africa and its relationship with environmental variability. *Global Change Biology* 21: 250–264. <https://doi.org/10.1111/gcb.12734>
- Taugourdeau S, Cofélas F, Bossoukpe M, Diatta O, Ndiaye O, Diedhiou A, N'Goran A, Audebert A, Faye E. 2023. Unmanned aerial vehicle outputs and associated field measurements of the herbaceous and tree layers of the Senegalese savannah. *African Journal of Ecology* 61: 730–735. <https://doi.org/10.1111/aje.13123>
- Taugourdeau S, Diedhiou A, Fassinou C, Bossoukpe M, Diatta O, N'Goran A, Audebert A, Ndiaye O, Diouf AA, Tagesson T, Fensholt R, Faye E. 2022. Estimating herbaceous aboveground biomass in sahelian rangelands using structure from motion data collected on the ground and by UAV. *Ecology and Evolution* 12: 1–17. <https://doi.org/10.1002/ece3.8867>
- Théau J, Gavelle E, Ménard P. 2020. Crop scouting using UAV imagery: a case study for potatoes. *Journal of Unmanned Vehicle Systems* 8: 99–118. <https://doi.org/10.1139/juvs-2019-0009>
- Umutoni C, Ayantunde AA, Sawadogo GJ. 2015. Evaluation of feed resources in mixed crop-livestock systems in Sudano-Sahelian Zone of Mali in West Africa. *International Journal of Livestock Research* 5: 27–36. <https://doi.org/10.5455/ijlr.20150813090546>
- Vera-Velez R, Grover SA, Bischoff BK, Carlyle CN, Lamb EG. 2023. Wildfire-grazing impact on forage quality assessed with near-infrared spectroscopy and generalized partial least squares regression. *Rangeland Ecology and Management* 87: 132–140. <https://doi.org/10.1016/j.rama.2023.01.003>
- Visockiene S, Puziene JR, Stanionis A, Tumeliene E. 2016. Unmanned aerial vehicles for photogrammetry: analysis of orthophoto images over the territory of Lithuania. *International Journal of Aerospace Engineering* 2016: 1–9. <https://doi.org/10.1155/2016/4141037>
- Wang H, Feng C, Li X, Yang Y, Zhang Y, Su J, Luo D, Wei D, He Y. 2024. Plant species diversity assessment in the temperate grassland region of china using UAV hyperspectral remote sensing. *Diversity* 16: 775. <https://doi.org/10.3390/d16120775>
- Wieckowski A, Vestin P, Ardö J, Roupsard O, Ndiaye O, Diatta O, Ba S, Agbohessou Y, Fensholt R, Verbruggen W, Hailu H, Tagesson T. 2024. Eddy covariance measurements reveal a decreased carbon sequestration strength 2010 – 2022 in an African semiarid savanna. *Global Change Biology* 30: 1–18. <https://doi.org/10.1111/gcb.17509>
- Yang G, Liu J, Zhao C, Li Z, Huang Y, Yu H, Xu B, et al. (2017) Unmanned aerial vehicle remote sensing for field-based crop phenotyping: current status and perspectives. *Frontiers in Plant Science* 8: 1111. <https://doi.org/10.3389/fpls.2017.01111>

- Yeom J, Jung J, Chang A, Ashapure A, Maeda M, Maeda A, Landivar J. 2019. Comparison of vegetation indices derived from UAV data for differentiation of tillage effects in agriculture. *Remote Sensing* 11: 1548. <https://doi.org/10.3390/rs11131548>
- Zhang J, Okin GS, Zhou B, Karl JW. 2021. UAV-derived imagery for vegetation structure estimation in rangelands: validation and application. *Ecosphere* 12: e03830. <https://doi.org/10.1002/ecs2.3830>
- Zhu X, Xinyu C, Ma L, Liu W. 2024. UAV and satellite synergies for mapping grassland aboveground biomass in Hulunbuir Meadow Steppe. *Plants* 13: 1–19. <https://doi.org/10.3390/plants13071006>
- Zwick M, Cardoso JA, Gutiérrez-Zapata DM, Cerón-Muñoz M, Gutiérrez JF, Raab C, Jonsson N, Escobar M, Roberts K, Barrett B. 2024. Pixels to pasture: using machine learning and multispectral remote sensing to predict biomass and nutrient quality in tropical grasslands. *Remote Sensing Applications: Society and Environment* 36:1 01282. <https://doi.org/10.1016/j.rsase.2024.101282>